Negative correlation energy and valence alternation in amorphous selenium: An *in situ* optically induced ESR study

A. V. Kolobov*
Joint Research Center for Atom Technology–National Institute for Advanced Interdisciplinary Research, 1-1-4 Higashi, Tsukuba, Ibaraki 305, Japan
and Electrotechnical Laboratory, 1-1-4 Umezono, Tsukuba, Ibaraki 305, Japan

M. Kondo, H. Oyanagi, and A. Matsuda
Electrotechnical Laboratory, 1-1-4 Umezono, Tsukuba, Ibaraki 305, Japan

K. Tanaka
Joint Research Center for Atom Technology–National Institute for Advanced Interdisciplinary Research, 1-1-4 Higashi, Tsukuba, Ibaraki 305, Japan

(Received 30 January 1998; revised manuscript received 23 June 1998)

Two different kinds of electron spin resonance (ESR) signals, triclinic and isotropic, are observed in amorphous selenium under photoexcitation at 20 K with a concentration of up to 10^{20} cm^{-3}. ESR annealing behavior shows that isotropic centers are not stable and are converted into triclinic defects. The defects are identified as singly and triply coordinated Se defects. The results present experimental evidence for negative-U centers and valence alternation in amorphous selenium. The relationship between the photoinduced ESR and reversible photodarkening is discussed. [S0163-1829(98)07338-X]

I. INTRODUCTION

Amorphous semiconductors, being intrinsically metastable, undergo reversible changes under photoexcitation. Typical examples are the Staebler-Wronski effect in hydrogenated amorphous silicon (a-Si:H) (Ref. 1) and photostructural changes in amorphous chalcogenides (see Ref. 2 for a review). In addition, amorphous chalcogenides, of which amorphous selenium (a-Se) is the simplest representative, exhibit a number of other unique properties, such as pinning of the Fermi level in the middle of the forbidden gap (usually called the mobility gap in the case of amorphous semiconductors) due to a large density of states in the gap. At the same time they are characterized by high transparency in the infrared (IR) region and absence of an electron spin resonance (ESR) signal.[3] In order to explain these contradictory facts, a concept of defects with negative correlation energy (negative-U) favoring the formation of doubly occupied states was suggested.[4] This model was developed further in Ref. 5, which suggested that dangling bonds (the main defects in a unielement material such as selenium) are charged according to the exothermic reaction

$$2D^0 \rightarrow D^+ + D^-, \tag{1}$$

where D denotes a dangling bond and superscripts correspond to the charge of the defect. At about the same time it was suggested[6] that the valence of defects change following the change in the charge. This is possible because of the presence of lone-pair (LP) electrons in chalcogens. The suggested reaction in which a *pair* of charged defects is formed is as follows:

$$2C_1^0 \rightarrow C_3^+ + C_1^-, \tag{2}$$

with C standing for chalcogen and subscripts corresponding to the coordination number (valence). This model, often called the valence-alternation-pair (VAP) model, is very efficient in explaining the majority of experimental results obtained for various chalcogenide glasses and is widely used.

Although all these models were initially suggested for elemental chalcogens such as selenium, there has so far been no *direct* experimental evidence for the existence of negative U and valence alternation in a-Se. The proof of the existence of charged defects is limited to observation of the dipolar activity in a-Se and some amorphous selenides by means of alternate current (ac) measurements.[7] However, no proof has ever been found that valence alternation does accompany bond breaking. The experimental proof for negative U in compound chalcogenides is the appearance of a strong electron spin resonance signal under light excitation (up to 10^{20} cm^{-3}, provided the light intensity is high enough).[8–10] However, such large densities of photoinduced unpaired spins were only reported for compound chalcogenides where calculations[11] also show the negative U.

For elemental selenium the situation is more complicated. Similar calculations for a-Se (Ref. 12) lead to the rather unexpected result that in a-Se the correlation energy is *positive*. The optically induced ESR observed experimentally, although giving strong support to the negative U, is not a final proof for negative U since the observed spin density was less than 10^{18} cm^{-3} (Ref. 8) and a-Se can easily have up to 10^{19} cm^{-3} (Ref. 3) impurities such as oxygen which can be responsible for the observed spin density. In addition to the possibility that the impurity itself is ESR active, it is also possible that inclusion of an impurity perturbs the a-Se network and the observed ESR signal, although coming from selenium species may originate in the vicinity of impurities thus being caused by their presence.

It is thus evident that the concepts of negative U and valence alternation in a-Se, which are the key issues of the widely used VAP model, lack reliable experimental evidence. In this paper we report the results of an *in situ* optically induced ESR study which present direct experimental evidence for negative U and valence alternation in a-Se. Preliminary results have been published elsewhere.[13]

II. EXPERIMENT

The samples for ESR measurements were a-Se films ($\sim$5 μm thick) deposited onto ESR-grade quartz substrates. The samples were prepared by thermal evaporation of 5N bulk selenium onto silica-glass and aluminum-foil substrates and kept at room temperature for at least 48 h to remove the irreversible component of the photoinduced structural change which is present in as-evaporated films.[2]

The sample was sealed in a quartz tube filled with helium. The measurements were carried out at 20 K both in the dark and under photoexcitation. The microwave power used was 1 mW, and care was taken to avoid signal saturation due to high microwave power. The photoexcitation using Ar-ion laser ($\lambda = 514.5$ nm) was performed at 20 K with an intensity at the sample surface of 50 mW/cm^2. To identify the origin of the ESR centers, we studied the kinetics of both the creation and the annealing of the optically induced ESR centers. The isochronal annealings for 20 min at elevated temperatures were carried out and ESR spectra were measured each time after cooling the sample back to 20 K. This experiment was done in order to discriminate between ESR signals due to centers with different creation and annealing behaviors. The intensity was calculated from the double integral of the resonance line, and the absolute value was calibrated using a standard sample (''strong pitch'') whose spin density is known.

To make sure that the observed ESR signal is intrinsic to a-Se and not caused by impurities, care was taken that concentration of impurities was lower than the observed photoinduced spin density.[13]

III. RESULTS

In the dark, no ESR signal was observed. However, photoexcitation resulted in a clearly observable signal. An ESR spectrum taken at 20 K is shown in Fig. 1 (top curve). In the first irradiation cycle for a sample cooled down from room temperature, the ESR signal increases slowly with light exposure (Fig. 2, closed circles) and its intensity levels off after $\sim$2 h of exposure (the saturated value is shown by a closed circle at the top right-hand side of the figure). Figure 3 shows ESR spectra measured after 2 min and 4 h of irradiation (at 50 K). It can be seen that the line shape is essentially the same for the two data sets despite quite different irradiation times. Since the optically induced ESR centers are frozen in at 20 K, the ESR signal is maintained even after the excitation light is turned off. Annealing above 150 K for 20 min destroys the ESR centers.

In the subsequent irradiation cycle for a sample previously irradiated at 20 K for several hours and then annealed at $T > 150$ K, the evolution of the ESR signal (measured at 20 K) occurs more rapidly than that in the first cycle, as shown in Fig. 2. The ESR signal saturates much faster while the line shape is identical to that observed in the first cycle. The sequence of curves shown in the figure corresponds to different annealing temperatures (indicated to the right of each curve). Two components, fast and slow, are seen in the curves. The faster component is more strongly pronounced for lower annealing temperatures and it gradually decreases as the sample is annealed at higher temperatures. Annealing at room temperature completely recovers the initial state of the sample. It is also seen that at the second stage the rate at which the ESR signal increases is independent of the previous treatment as evidenced by the essentially identical slopes of the dashed lines approximating the ESR increase rate.

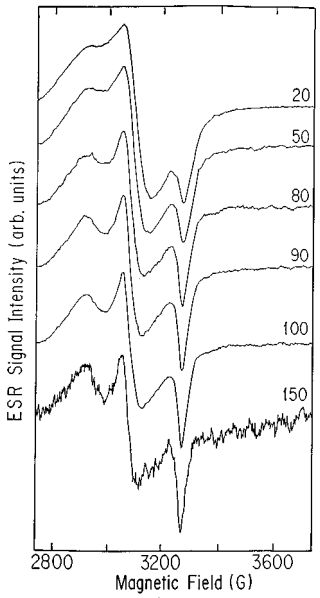

FIG. 1. Observed total ESR spectrum taken at 20 K (top) and its temperature evolution after annealing at temperatures indicated next to each curve for 20 min. The measurements were all done at 20 K.

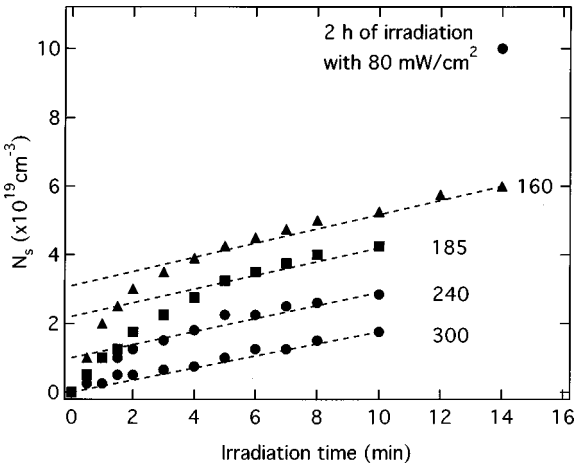

FIG. 2. Kinetics of light-induced spin density at 20 K in the starting film (bottom) and in the film previously irradiated for several hours at 20 K and then annealed for 20 min at $T > 160$ K (three upper curves). The annealing temperature is indicated next to each curve. The closed circle in the top-right corner corresponds to the spin density after 2 h of irradiation. Dashed lines approximate the slow-rate stage of the kinetics.

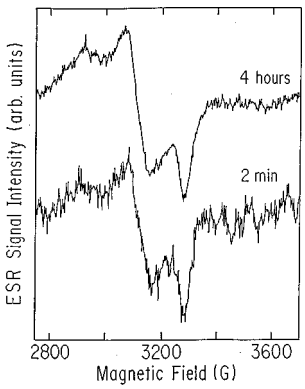

FIG. 3. ESR spectra taken after 2 min and 4 h of irradiation at 50 K.

In the isochronal annealing experiments, the results of which are shown in Fig. 1, it is seen that the line shape of the ESR changes at successive annealing steps for $T_a<100$ K, while no change occurs for higher temperatures ($T_a>100$ K). This implies that at $T<100$ K two or more centers coexist while at $T>100$ K only one center exists. The line shape of this center (Fig. 1; spectra taken after annealing at 100 and 150 K) reveals the characteristics of a triclinic center with its principal values of g tensors being 2.22, 2.099, and 1.983. These values are in good agreement with those in the previous work [2.16, 2.09, and 2.00 (Ref. 8)] except that the spin density is much higher in the present study. The spin density of the triclinic center induced at 20 K is estimated to be 5.5×10^{19} cm^{-3}. Assuming that the line shape of the triclinic component is always the same as that at $T_a>100$ K, the signal for lower T_a can be deconvoluted into the triclinic component and a remaining rather broad and structureless component. The broad component obtained from the spectra recorded at 20 and 70 K is shown in Fig. 4. Small structures in the resonance line can be seen. Although we cannot rule out a possibility that this structure is an artifact arising from the deconvolution process, we would like to point out that the same structure is observed for all data taken for $T<100$ K at almost symmetric position with respect to the resonance position.

In this paper, the triclinic center is referred to as the T center and the remaining center as the B center. The g value and the linewidth for the B center are 2.09 and ~150 G,

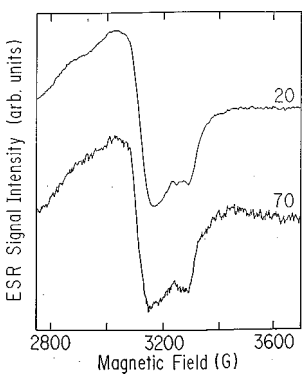

FIG. 4. Isotropic (deconvoluted) component of the ESR signal. Results of deconvolution for spectra taken at 20 and 70 K are shown.

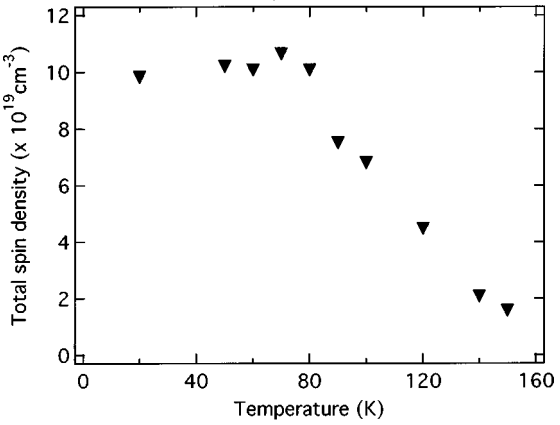

FIG. 5. Temperature behavior of the total number of photoinduced spins.

respectively, and the spin density at 20 K is 5.3×10^{19} cm^{-3}. It is of interest to note that the starting concentrations of the two kinds of photoinduced defects are the same within experimental accuracy.

The annealing temperature dependence of the spin density of the two centers (T and B centers) has been described in detail elsewhere (Ref. 13, Fig. 3). In the region $T_a<100$ K, it was found that these two components show complementary behavior, namely, a decrease in the concentration of B centers concurrent with an increase in the concentration of T centers. This implies that the B centers *are converted* into the T centers with increasing temperature and that the T center is more stable than the B center. For $T_a>100$ K, only T centers are observed, decreasing its intensity with increasing temperature, and finally for $T_a>150$ K the ESR signal is completely annihilated. Thus, light exposure creates two different kinds of metastable defects, namely, T and B centers, and with increasing temperature a conversion from B to T centers takes place. An estimate of energy barrier between the two states (B and T) gives a value of about 10–30 meV.

Figure 5 shows the temperature dependence of *total* spin density on annealing of the irradiated sample. Unlike the behavior of each of the two components shown in Fig. 3 of Ref. 13, the total concentration does not change in the temperature range of 20 to 80 K, after which it decreases and disappears at around 160 K.

In order to check whether the defect transformation is accompanied by a change in coordination, we performed an *in situ* extended x-ray-absorption fine structure (EXAFS) experiment which is a unique technique to get direct information on the local structure. Results of this study will be published elsewhere.[14]

IV. DISCUSSION

The fact that there is an optically induced ESR signal while no signal is observed in the dark implies that the defects acquire unpaired spins in the excited states while in the ground state there are no unpaired spins. This is the situation characteristic of centers with negative U. The observed high density of spins (~10^{20} cm^{-3}) clearly shows that the signal is not caused by impurities, e.g., oxygen, but is intrinsic to the nature of a-Se. This result gives direct evidence of nega-

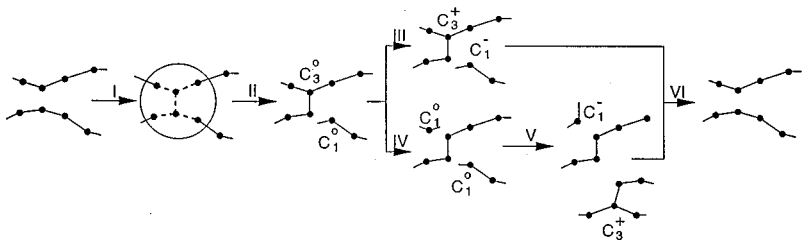

FIG. 6. Schematic representation of the reversible photostructural change in *a*-Se. Under photoexcitation dynamic interchain bonds (shown by dashed lines in the encircled area) are formed (step I) which break into a neutral (ESR-active) VAP (step II). Two different possibilities for stabilization of neutral defects include direct charge transfer (step III) and formation of charged VAP via intermediate bond breaking (steps IV and V). Annealing at room temperature leads to recovery of initial structure (step VI).

tive U in this material. An important point is that the starting concentrations of the two kinds of photoinduced defects are the same, which strongly suggests that the defects are created *in pairs*. The same line shape at the initial (2 min) and final (4 h) stages of irradiation obtained at a different temperature of 50 K (Fig. 3) demonstrates that this is always the case.

We shall now discuss the ESR annealing behavior. It is obvious from Fig. 1 that at temperatures higher than 100 K only one ESR center exists while at lower temperatures two different centers coexist. Previously,[8] it was suggested that the more stable triclinic center arises from a localized hole on the Se site, because the g shift is positive and large, but the authors did not discuss the specific defect structure such as VAP. If the T center is the C_1^0 center, the unpaired electron is located in one of the nonbonding orbitals while other orbitals are filled. Therefore, this center is holelike, which is consistent with the sign of the g shift. On the assumption of sp hybridization for singly bonded radicals with a fractional s character of ~ 0.4 the principal values of the g tensor have been calculated to be $g_1=2.22$, $g_2=2.075$, and $g_3=2.0023$.[15] [Similar values have been obtained in a different calculation: $g_1=2.238$, $g_2=2.104$, and $g_3=2.002$ (Ref. 16)]. These values are in good agreement with our experimental data. We thus conclude[13] that the T center is a neutral dangling bond, C_1^0. In addition, it is reasonable to expect that a singly coordinated atom will be more relaxed; thus the anisotropy of the center should clearly appear while a triply coordinated center will be more distorted due to the network strain and its structure should be smeared out. In the C_3^0 center, the electron is in the antibonding orbital. Degeneracy of three bonding orbitals will be lifted as a consequence of the lattice distortion. Therefore it is expected that the C_3^0 center will show less anisotropy (than C_1^0) and a more broadened spectrum due to the disorder. The small structures observed in the line shape of the isotropic center can be caused by hyperfine doublets due to ^{77}Se ($I=\frac{1}{2}$, 7.58% abundance).[13]

A question may arise as to why the average g values are practically the same for the two quite different defects. One of the possibilities would be that the three bonds of the overcoordinated defect are not static but rather dynamic. In such a case, the signal from such a center should be similar to that of a singly coordinated defect but should have less structure. Also, this configuration should be rather unstable and should easily decay into a singly coordinated defect and a twofold-coordinated selenium atom forming part of a selenium chain. The fact that the isotropic center decays at higher temperatures and *is converted* into the monoclinic defect gives support to this argument. This process can be expressed by the reaction

$$C_3^0 \rightarrow C_1^0. \tag{3}$$

The estimated energy barrier for the defect conversion of about 10 meV is indeed very small and agrees well with the results of calculations[17] which have shown that a threefold-coordinated defect is unstable and is transformed into a singly coordinated defect. We thus conclude that the triclinic center is a singly coordinated defect and the isotropic center is a triply coordinated defect. As already mentioned, this conclusion agrees well with the results of calculations made[17] but contradicts a simple idea of the VAP model[6] which suggested that a triply coordinated neutral defect was more stable.

Now we turn to the kinetics of optically induced ESR. Similar behavior was reported earlier for As_2S_3 (Ref. 9) and it was concluded that the fast component represented the *excitation* of already existing defects, while the slow component was related to the *creation* of new defects. We agree with this interpretation. Our previous EXAFS studies of photostructural changes in *a*-Se (Ref. 18) have shown that under photoexcitation a number of dynamic interchain bonds are formed making a certain proportion (up to 6%) of selenium atoms threefold coordinated (Fig. 6, step I). These light-induced extra bonds are essentially dynamic, which is marked by dashed lines representing covalent bonds in the figure, and break (step II), resulting in unpaired spins as is seen from the figure. We can describe this process by the following reaction:

$$2C_2^0 \rightarrow 2C_2^* \rightarrow 2C_3^0 \rightarrow C_3^0 + C_1^0. \tag{4}$$

At the same time light irradiation excites already existing defects as shown by the reactions

$$\begin{aligned} C_3^+ &\rightarrow C_3^0, \\ C_1^- &\rightarrow C_1^0. \end{aligned} \tag{5}$$

The latter reactions do not require any bond rearrangement and are much faster than the former reaction which involves bond rearrangement. Both reactions take place simultaneously but since the number of intrinsic (dark) defects is smaller than that of light-induced defects, reaction (3) dominates and we can only observe the slow component in the annealed sample.

Annealing at $T>160$ K brings the defects to a more stable (for negative-U centers) charged state according to reaction (2). When secondary irradiation takes place there are already a large number of charged defects and it is only necessary to excite them in order to create ESR-active centers. This explains why the ESR grows at a much faster rate in the second irradiation cycle. At the same time the photoinduced defects recombine with the number of recombined defects increasing with the annealing temperature. This results in a decrease of the fast component observed in the second irradiation.

We will now discuss the process taking place at $T>160$ K, i.e., the conversion of neutral defects into charged defects, in more detail. One possibility is that the defect pair is stabilized as it is by a simple charge transfer without any change in the bonding topology (Fig. 6, step III). This process would result in the formation of a charged valence alternation pair. Another possibility is that a triply coordinated defect decays first into a normally coordinated atom and a more stable neutral undercoordinated defect with a pair of neutral dangling bonds (Fig. 6, step IV) further transformed into a charged valence alternation pair (step V). Although a naive consideration would suggest that the first process is more likely to take place, the experimental data demonstrate that this is not the case. Indeed, should the process be taking place by direct stabilization of a VAP by a charge transfer, then the two ESR signals should disappear in pairs, which is clearly not the case: up to 80 K (and this is the temperature at which C_3^0 are annealed out), the total concentration of ESR centers remains constant, not exhibiting any decrease (Fig. 6). This clearly shows that direct stabilization of VAP's by the charge transfer has a very low probability. A possible explanation could be different energy barrier heights for the two pathways. Thus even though the process involving the bond breaking may seem longer the barrier height on this pathway being lower would explain its higher probability.

Another implication from this result is that electron pairing is only possible via intermediate bond breaking. This could probably account for why the result of theoretical calculations obtained in Ref. 12 has led the authors to a conclusion that the correlation energy for selenium was positive.

V. RELATIONSHIP BETWEEN PHOTOINDUCED ESR AND REVERSIBLE PHOTOSTRUCTURAL CHANGE (PHOTODARKENING)

In this section we would like to discuss the relationship between the photoinduced ESR and reversible photostructural change which is characteristic of amorphous chalcogenides.[2] After the introduction of the VAP model it was suggested[19] that photoinduced charged defects created in large concentration were responsible for the photodarkening. However, in a later study of photoinduced ESR in As_2S_3,[10] it was shown that the temperature dependence of the photodarkening, which is a manifestation of the photostructural change, and that of photoinduced ESR are quite different. While photoinduced ESR is annealed out at about 200 K the photodarkening is stable to much higher temperatures. This result has led the authors of Ref. 10 to a conclusion that the mechanisms of the photodarkening and photoinduced ESR are different and this point of view seemed to have dominated. Below we demonstrate that the earlier suggestion,

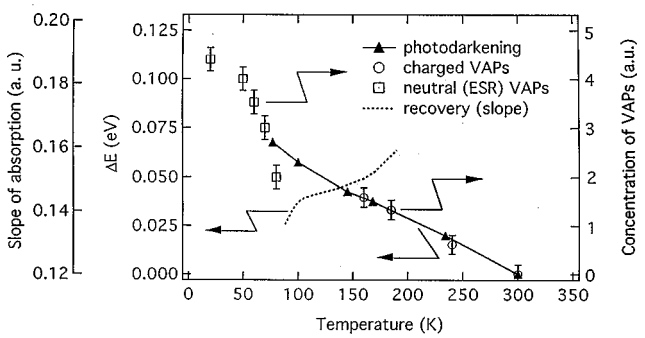

FIG. 7. Temperature dependencies for the photodarkening (absorption edge shift, data taken from Ref. 20, solid line connecting closed triangles), concentrations of charged VAP's (open circles) and neutral VAP's (open squares), and recovery of the photodarkening (slope of the absorption edge, data taken from Ref. 21, dashed line).

namely, that photostructural change and creation of photoinduced VAP's are closely correlated, is likely to be more correct.

It is important to realize that after annealing at temperatures $T>160$ K *photocreated VAP's do not disappear*. What disappears is the ESR signal but this is related not to the presence or absence of VAP's but to their charge state. The defects become charged and hence ESR *inactive* but they are still there, which is clearly evidenced by the presence of the faster component in the ESR kinetics in the secondary irradiation process. A relative amplitude of the fast component is a measure of the concentration of charged VAP's. In Fig. 7 we show temperature dependencies for the photodarkening in a-Se (the data taken from Ref. 20) and those for the concentration of *charged VAP's*. The two curves are normalized in such a way that the first point (at 160 K) for the temperature dependence of the VAP's concentration is placed onto the curve for the photodarkening dependence. An excellent agreement between the temperature behaviors of the two effects is obvious.

Furthermore, we can also add to the plot concentrations of *neutral (ESR-active) VAP's* obtained from Ref. 13. The concentration of neutral VAP's is put on the same scale as the charged VAP's. One can easily see that this concentration also correlates well with the magnitude of the photodarkening. A slight difference between the temperature behaviors of the photodarkening and concentration of neutral VAP's at around 90 K could be caused by the fact that disappearance of a charged VAP means disappearance of (photoinduced) defects while disappearance of a neutral VAP does not mean disappearance of defects: the singly coordinated defect remains unchanged and a triply coordinated defect does not disappear as such but is converted into another kind of defect, i.e., a dangling-bond pair (DBP) is formed. Since lattice distortions around singly coordinated defects also contribute to the photoinduced change in the optical absorption, although to a lesser degree than those around threefold-coordinated defects, the change in the photoinduced absorption should be smaller than the decrease in concentration of charged VAP's, in agreement with the data shown in Fig. 7.

The correlation between photoinduced ESR and photodarkening is further evidenced if we consider the result of a

thorough investigation of the temperature dependence of the recovery of initial parameters (the slope of the absorption edge) in the photodarkened *a*-Se reported in Ref. 21 and shown in Fig. 7 as a dashed line. One can clearly see that there are two characteristic temperatures at which the slopes in annealing of the photodarkening in *a*-Se change. These temperatures are in good agreement with the characteristic temperatures of 90 and 160 K in the photoinduced ESR, demonstrating that a change in the nature of photoinduced defects (charge or coordination) is reflected in the optical absorption. A slower recovery rate in the temperature range between 100 and 160 K can be understood on the basis of the present study. Indeed, at lower temperatures when a strained bond subtended at a threefold-coordinated atom breaks, rather large lattice relaxation becomes possible (faster change in recovery of the slope). In the temperature range of 90 to 160 K, dangling bonds get charged and a positively charged one forms an extra bond to a neighboring chain utilizing lone-pair electrons of the latter. The lattice relaxation accompanying this process is likely to be smaller (slower recovery rate). Finally at $T>160$ K charged VAP's recombine into normally coordinated atoms which involves rather large lattice relaxation and this manifests itself as an increase in the recovery rate.

We can thus conclude that the photodarkening is closely correlated with the concentration of VAP's, either neutral or charged. The underlying mechanism is believed to be the following. In the annealed state, the lone-pair orbitals of selenium, forming the top of the valence band, are oriented perpendicular to each other in order to minimize the energy. *Any change* in the atomic positions, such as the creation or VAP defects (either neutral and hence ESR active or charged and not detectable by ESR), results not only in displacements of the particular atoms involved but also in displacements of their neighbors from their original positions. This increases the repulsive interaction between the LP electrons and results in a shift of the top of the valence band upwards in energy thus leading to a decrease in the forbidden gap, i.e., photodarkening. We thus believe that photoinduced VAP's are like seeds around which a structural change takes place, causing the photodarkening. The electric field, introduced by charged VAP's present in high concentration, may also play a certain role, for example, through its effect on the excitonic absorption edge as discussed by Dow and Redfield.[22]

We believe that the mechanism is essentially the same in elemental selenium and in compound chalcogenides, the process in the latter group being more complicated since, in addition to coordination defects, stoichiometric defects (''wrong bonds'') can also be induced in the material through the formation of dynamic interchalcogen bonds.[23,24]

VI. CONCLUSION

The results of the present study give direct experimental evidence for the negative *U* and valence alternation in *a*-Se.

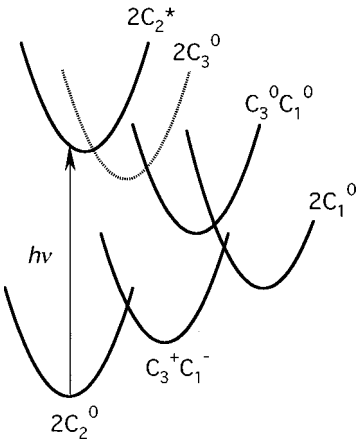

FIG. 8. Configuration diagram illustrating the reversible photostructural change. The corresponding atomic configurations are indicated next to each curve.

In a previous paper[18] we reported creation of dynamic bonds between selenium chains under photoexcitation. The results presented in this paper enable us to understand the details of the structural transformation following the excitation step. These transformations proceed as follows. After the photoexcitation bond breaking takes place at threefold-coordinated atoms resulting in a pair of ESR-active centers. One of the defects is singly coordinated and the other one is triply coordinated. This neutral VAP is not stabilized by direct charge transfer. Instead, the triply coordinated neutral defect is converted into another singly coordinated defect at temperatures around 90 K and a DBP is formed. At higher temperature, pairs of singly coordinated neutral defects (DBP) are transformed into pairs of charged defects, one of which becomes threefold coordinated, i.e., a charged VAP is formed. At yet higher temperature, charged defects recombine and the initial structure of the material is restored. The whole process is summarized in Fig. 6. A configuration diagram illustrating the structural changes during the reversible photodarkening cycle is shown in Fig. 8.

Based on close correlation between the concentration of VAP pairs and the photodarkening we conclude that the photodarkening is caused by photoinduced creation of valence-alternation pairs which act as seeds for lattice distortion responsible for the photodarkening.

ACKNOWLEDGMENTS

R. Durny's participation in the initial stage of this study is appreciated. The authors would like to acknowledge useful discussions with J. Isoya and S. Yamasaki. This work, partly supported by NEDO, was performed in the Joint Research Center for Atom Technology (JRCAT) under the joint research agreement between the National Institute for Advanced Interdisciplinary Research (NAIR) and the Angstrom Technology Partnership (ATP).

*On leave from A. F. Ioffe Physico-Technical Institute, St Petersburg, Russia.
[1] D. L. Staebler and C. R. Wronski, Appl. Phys. Lett. **31**, 292 (1977).
[2] K. Shimakawa, A. V. Kolobov, and S. R. Elliott, Adv. Phys. **44**, 475 (1995).
[3] N. F. Mott and E. A. Davis, *Electronic Processes in Non-Crystalline Materials*, 2nd ed. (Clarendon, Oxford, 1979).
[4] P. W. Anderson, Phys. Rev. Lett. **34**, 953 (1975).
[5] R. A. Street and N. F. Mott, Phys. Rev. Lett. **35**, 1293 (1975).
[6] M. Kastner, D. Adler, and H. Fritzsche, Phys. Rev. Lett. **37**, 1504 (1976).
[7] M. Abkowitz and D. M. Pai, Phys. Rev. Lett. **24**, 1412 (1977).
[8] S. G. Bishop, U. Strom, and P. C. Taylor, Phys. Rev. Lett. **34**, 1346 (1975).
[9] D. K. Biegelsen and R. A. Street, Phys. Rev. Lett. **44**, 803 (1980).
[10] J. Hautala, W. D. Ohlsen, and P. C. Taylor, Phys. Rev. B **38**, 11 048 (1988).
[11] D. Vanderbilt and J. D. Joannopoulos, Phys. Rev. B **23**, 2596 (1981).
[12] D. Vanderbilt and J. D. Joannopoulos, Phys. Rev. Lett. **49**, 823 (1982).
[13] A. V. Kolobov, M. Kondo, H. Oyanagi, R. Durny, A. Matsuda, and K. Tanaka, Phys. Rev. B **56**, R485 (1997).
[14] A. V. Kolobov, H. Oyanagi, and K. Tanaka (unpublished).
[15] M. Abkowitz, J. Chem. Phys. **46**, 4537 (1967).
[16] H. Fukutome and A. Ikawa (private communication).
[17] D. Vanderbilt and J. D. Joannopoulos, Solid State Commun. **35**, 535 (1980).
[18] A. V. Kolobov, H. Oyanagi, K. Tanaka, and Ke Tanaka, Phys. Rev. B **55**, 726 (1997).
[19] R. A. Street, Solid State Commun. **24**, 363 (1977).
[20] Ke. Tanaka, J. Non-Cryst. Solids **59-60**, 925 (1984).
[21] R. Chang, Mater. Res. Bull. **2**, 145 (1967).
[22] J. D. Dow and D. Redfield, Phys. Rev. B **1**, 3358 (1970).
[23] M. Frumar, A. P. Firth, and A. E. Owen, Philos. Mag. B **50**, 463 (1984).
[24] A. V. Kolobov, K. Tanaka, and H. Oyanagi, Phys. Solid State **39**, 64 (1997).